Electro-chemical deposition of zinc oxide nanostructures by using two electrodes

B. A. Taleatu, A. Y. Fasasi, G. Di Santo, S. Bernstorff, A. Goldoni, M. Fanetti, L. Floreano, P. Borghetti, L. Casalis, B. Sanavio, and C. Castellarin-Cudia

Citation: AIP Advances **1**, 032147 (2011); doi: 10.1063/1.3633476

View online: http://dx.doi.org/10.1063/1.3633476

View Table of Contents: http://aip.scitation.org/toc/adv/1/3

Published by the American Institute of Physics

Electro-chemical deposition of zinc oxide nanostructures by using two electrodes

B. A. Taleatu,[1,2,3] A. Y. Fasasi,[2] G. Di Santo,[3] S. Bernstorff,[3] A. Goldoni,[3] M. Fanetti,[3,4] L. Floreano,[4] P. Borghetti,[5] L. Casalis,[3] B. Sanavio,[3] and C. Castellarin-Cudia[3]

[1]*Department of Physics, Obafemi Awolowo University Ile-Ife, Nigeria*
[2]*Centre for Energy Research and Development, O.A.U., Ile-Ife, Nigeria*
[3]*Sincrotrone Trieste. S.C.p.A., s.s 14 Km 163.5 in Area Science Park, 34149 Basovizza, Trieste, Italy*
[4]*Lab. TASC, IOM-CNR, s.s 14 Km 163.5 in Area Science Park, 34149 Basovizza, Trieste, Italy*
[5]*Dip. di Matematica e Fisica, Università Cattolica del Sacro Cuore, Via dei Musei 41, 25121 Brescia, Italy*

(Received 10 May 2011; accepted 26 July 2011; published online 24 August 2011)

One of the most viable ways to grow nanostructures is electro deposition. However, most electrodeposited samples are obtained by three-electrode electrochemical cell. We successfully use a much simpler two-electrode cell to grow different ZnO nanostructures from common chemical reagents. Concentration, pH of the electrolytes and growth parameters like potentials at the electrodes, are tailored to allow fast growth without complexity. Morphology and surface roughness are investigated by Scanning Electron and Air Force Microscopy (SEM and AFM) respectively, crystal structure by X-Ray Diffraction measurements (XRD) and ZnO stoichiometry by core level photoemission spectroscopy (XPS). [doi:10.1063/1.3633476]

I. INTRODUCTION

At present, much emphasis is put on the fabrication of metal oxide nanostructures due to their potential applications in the growing technologies such as optoelectronics, photovoltaics, electrochromic windows, chemical sensors and so on.[1] The ease in controlling the synthesis of ZnO at the nanoscale and the understanding of their physicochemical properties and electronic structure are crucial for the development of ZnO-based nanodevices.

ZnO is characterized by several useful properties. It has a wide band gap (3.3-3.4 eV), it exhibits a large exciton binding energy (60 meV), which is higher than the one for Si (14.7meV), GaN (26meV) and ZnS (37 meV), near UV-emission and transparent conductivity. These properties make ZnO a promising material in photovoltaic energy conversion. It has the ability to grow high quality film/crystal, having extremely low contents of impurities and lattice defects (e.g. stacking faults, dislocations and grain boundaries).[2] Furthermore due to the non centrosymmetric wurtzite structure of the ZnO crystal, these nanostructures have a piezoelectric character, while the net ionic charges of the Zn^{2+}-terminated facets and O^{2-}-terminated facets produces spontaneously a positively charged Zn-(0001) and negatively charged O-(000-1) polar surfaces along the c-axis. Because of these behavior they are useful in building electro-mechanical coupled sensors and transducers.[3] ZnO is also a bio-safe and bio-compatible material[4] therefore it can be directly used without coating. Lastly it has high-energy radiation stability which makes it very suitable for space applications.[5]

With these unique properties, ZnO is one of the most important nanomaterials for integration with microsystems and biotechnology, but the feasibility of ZnO for these applications is due also to

TABLE I. Preparation conditions of samples shown in fig 2

Sample (ZnO)	Electrolyte (0.2M)	Substrate	pH	Voltage (V)	Deposition Time (min)
a) ***corals***	$Zn(NO_3)_2$	ITO	7.0±0.1	2.50	6
b) ***flakes***	$Zn(NO_3)_2$	Au-Cr/Si	7.0±0.1	2.80	5
c) ***nanorods***	$Zn(NO_3)_2$	Si(111)	7.0±0.1	3.20	5
d) ***tetrahedral net***	$Zn(NO_3)_2$	Coated Si(111)	7.0±0.1	3.80	11
e) ***nanowalls***	$ZnCl_2$	ITO	7.0±0.1	2.48	15

the successful synthesis of diverse nanostructures.[6] For instance, high surface area ZnO nanocrystals such as nanotubes or nanorods can enhance photon-to-electron conversion efficiency.[7]

One of the most suitable techniques of producing nanostructures is electrochemical deposition. In most works, three-electrode electrochemical cells, having saturated calomel electrode (SCE) as reference electrode, have been widely employed for the growth since 1996.[8,9] In addition, a solution of potassium chloride (KCl) is often introduced as supporting electrolyte.[10] Indeed, apart from catalyzing the electrolytic reaction, the presence of KCl gives room for challenging the purity of the sample.

Only a few very recent works show the possibility of obtaining ZnO nanostructures by means of a two electrode electrochemical cell. None of them reports about the possibility of tailoring the nanostructure formation only by changing the cell parameters and keeping constant the solution characteristics.[11,12]

We report in this communication a very simple, almost costless, method to grow ZnO nanocrystals synthesized by a two-electrode cell. The electrolytes are prepared from common chemical reagents in usual way and no supporting electrolyte is used. We also investigate the influence of substrate properties and deposition parameters on ZnO crystallinity and electronic properties, in particular regarding the cell conditions.

II. EXPERIMENTAL

To prepare the electrolyte, all chemicals are analytical grade (99.9% purity, Sigma-Aldrich) and they are used as received. Two different reacting solutions are prepared as indicated in Table I. $Zn(NO_3)_2$ electrolyte is obtained by dissolving 11.90 g of hydrated zinc trioxonitrate (V) salt (Zn(NO3)2.6H2O) in 200 ml standard flask. 5.45 g of anhydrous zinc chloride ($ZnCl_2$) is dissolved to 200 ml mark and heated at 60 ^oC for about 10 minutes to yield a clear $ZnCl_2$ solution. All the reacting masses result in 0.2M solution in each case. They are then kept for at least 24hrs before use.

Three types of conductive substrates are used for the deposition to study the influence of different materials on the structure and morphology of the ZnO nanostructures: Indium Tin Oxide (ITO), Si(111) and Au-Cr/Si(100). Both ITO and Si(111) are obtained from stock, but the Au-Cr/Si(100) is prepared by vacuum evaporation under standard conditions. A 200 Å thick film of chromium is first evaporated onto a Si(100) wafer to provide adhesion and then 1000 Å of gold is deposited atop the chromium.[13] Prior to deposition, all the substrates are cleaned in ultrasonic bath, rinsed with millipore water and dried in air. After this, Si(111) wafer is treated in dilute HNO_3 solution for about 10 minutes to remove the oxide layer on the surface, washed again with millipore water and finally dried with nitrogen. The ZnO electrochemical growth is performed on ZnO coated Si(111) too. A clean Si(111) wafer, is first coated in a solution (bath) containing 0.2M zinc acetate dehydrate ($Zn(C2H3O2)2 \cdot 2H2O$), 0.2M acetic acid (C2H4O2, 99.5% Sigma-Aldrich) and 0.1M ethanol (C2H6O, 99.8% Sigma-Aldrich) in ratio 2:1:1 by volume. The coating is carried out in one hour at a bath temperature of 62 ^oC. The resulting thin layer of ZnO on silicon is washed with millipore water, dried in a tubular furnace and used for the electrodeposition.

The two-electrode electrochemical cell shown in Fig 1 is used to grow the ZnO nanostructures and all the experiments are performed at room temperature. In the cell set up, the substrate

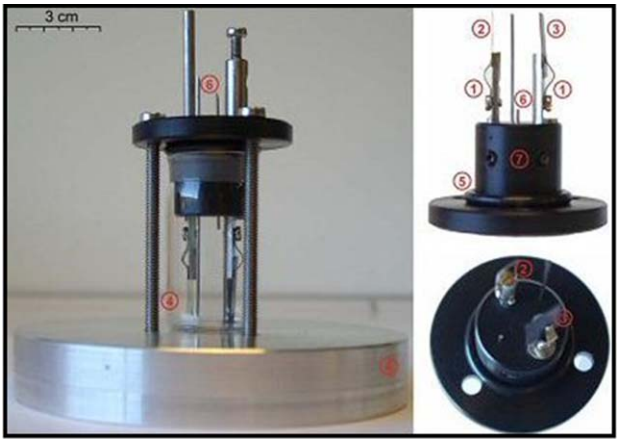

FIG. 1. Electrochemical cell used for ZnO growth. (1) electron holders with clamps, stainless steel, variable in height, (2) working electrode: substrate for ZnO growth. (3) counter electrode: graphite. (4) glass container. (5) rubber gasket. (6) inlet tubes and holes for gases and liquids. (7) screws for adjusting electrode older height. (8) aluminium stand.

acts as the working electrode while a piece of graphite (17.4 mm x 25.0mm x 39.5 mm) as the counter electrode. The two electrodes are held firmly to the holders (separation of 32.28 mm) with the coating surface of the working electrode facing directly the counter electrode. The electrolyte in each case is filled into the cell through a steel tube and the filling level is adjusted by a syringe. The cell is sealed by a rubber gasket held between the glass container and the stopper. The cell is then connected to a GPS-30300 power supply and a digital multimeter used to attain stabilized power with sensitive current and voltage modes. The deposition is carried out within short times by selectively applying a voltage (see Table I) at the counter electrode. We do not use any supporting electrolyte, but the growth is determined by the choice of potential and solution concentration. In a typical nucleation, when the cathodic potential is applied, hydroxyl ions are electrochemically generated at the surface of the working electrode and ZnO is precipitated from the reduction of molecular oxygen in the presence of Zn precursor.[14] At this juncture, it is noteworthy that we successfully avoid reference electrode (third electrode in the case of three-electrode cell) and we also overcome the complexity that might arise due to supporting electrolyte. Our two-electrode electrochemical cell allows good flexibility of tuning the height and the relative orientation of the electrodes as well as selecting desired voltage to obtain fast growth and good coverage.

Shape and distribution of the grown ZnO crystals across the substrates are observed by morphological studies using a scanning electron microscope (Zeiss Supra 40 with Gemini Column) characterized by a nominal resolution of 1nm at 10KeV and electron beam energy ranged from 0.1-30 KeV. SEM measurements are performed at the CNR-IOM national laboratory TASC, in Trieste, Italy. At the Nanostructure Laboratory of Sincrotrone Trieste, Italy, a complementary study of the growth height and roughness is carried out using a PSIA XE-100 AFM microscope and all the experiments are performed in contact mode. To determine the crystal structure and the composition of the ZnO and to compare the results with those already reported in literature, based on different growth techniques, XRD and XPS studies are carried out at the Sincrotrone Trieste. Diffraction measurements are performed at SAXS beamline, while photoemission experiments at ALOISA beamline and at Micro & Nano Carbon Laboratory. At the SAXS beamline the diffraction data are collected at 8 keV photon energy with a 1D (Gabriel type) gas detector covering an angular range 2 theta from 22° to 74°. At ALOISA beamline the photoemission spectra are taken by means of a hemispherical electron energy analyzer operated at 100 meV resolution and $\pm 1^\circ$ angular resolution while at Micro & Nano Carbon Laboratory the experiments are done using a VG Escalab MKII apparatus provided with a Mg Kα X-ray source and the XPS spectra collected with a 150 mm spherical electron energy analyzer with a total resolution of 1.2 eV.

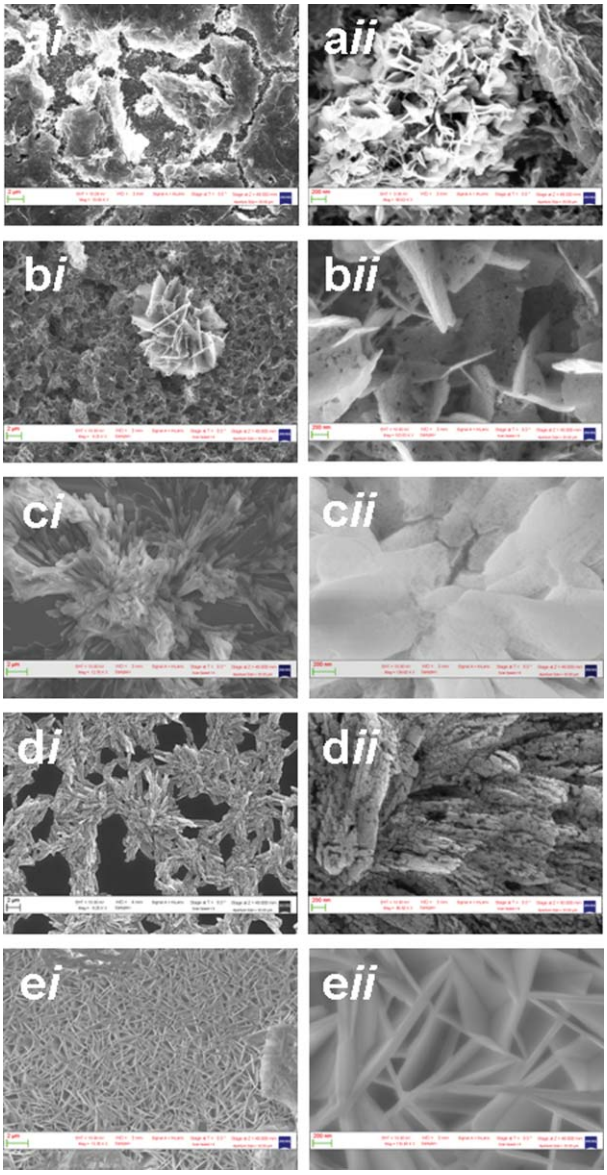

FIG. 2. SEM images of corals (a), flakes (b), nanorods (c), tetrahedral net (d), nanowalls (e). Scale bar in "*i*" figures is 2μm. Scale bar in "*ii*" figures is 200nm

III. RESULTS AND DISCUSSION

A. SEM

Table I shows a summary of the prepared samples. It reports the used electrolyte and substrate and the growth conditions, while Fig. 2 shows the corresponding SEM images.

ZnO nanostructures shown in Fig 2(a)–2(d) are obtained using $Zn(NO_3)_2$ as electrolyte, while the one in Fig 2(e) is prepared using $ZnCl_2$. Different substrates and electrode potentials are applied in the growth process in which the $Zn(NO_3)_2$ electrolyte is used (Fig 2(a)–2(d)), while the sample shown in Fig 2(e) is prepared using the same substrate and the same growth conditions applied to the sample in Fig 2(a), a part for the electrolyte. In any case the pH of the electrolyte solution is kept mainly constant at 7.

As a result we obtain different types of ZnO nanostructures, confirming the feasibility to have a lot of different growth types. They are different in structure and shapes, depending on

the nature of the electrolyte, on the experimental conditions and on the substrate, but the choice of equal concentration (0.2M) for all the electrolytes allows to understand the influence on the growth of substrate's conductivity, applied voltage and deposition rate. The two-electrode cell offers the advantages of simplicity and flexibility of the growth conditions. The results of morphology and structural studies show that the grown samples compare well with those reported in literature obtained using three-electrode cells, supporting electrolyte and some other growth techniques.[15,16] To simplify the discussion on the morphologies and ensure effective comparison, we classify the samples according to the used electrolyte and then describe the growth distribution and coverage with preference to the substrate.

Using zinc nitrate electrolyte we obtain four different ZnO nanostructures. Fig 2(a) shows at different magnification a ZnO "coral" like structure, obtained on plain ITO substrate. At low magnification (Fig 2(a)(i)) uniformly distributed crystalline particles are observed. When viewed at high magnification (Fig 2(a)(ii)) it can be seen that the crystal is an agglomerate of leaves-like structures and the neighboring particles merging to form one. A good inference that can be drawn here is that ZnO particles grow from the solution to form corals in a continuous or repeated manner, which fuse together to pave way for the emergence of another combination. In Fig 2(b), a "flakes" like structure of ZnO grown on Au-Cr/Si substrate is presented. A look at the low magnification image (Fig 2(b)(i)) reveals that also in this sample the "flakes" like objects are well distributed across the substrate. Furthermore it can be seen in the high-resolution image (Fig 2(b)(ii)) that the structure is filled with pores. The formation of pores can be attributed to the enhanced growth height or roughness of the sample. However these pores do not alter the structure of the ZnO as it is visible in the image Fig 2(b)(ii), which shows the patterned grains of the sample that are characteristics of the wurtzite structure. Formation of pores in ZnO structures was reported by many authors. In the work of Beek *et al.*,[17] they observed with both SEM and AFM techniques that an increase in roughness, due to high ZnO content, leads to formation of large pores without any change in morphology. SEM images of "rod" like ZnO nanostructures deposited on Si(111) wafer are shown in Fig 2(c). The closed-tip discs (Fig 2(c)(i)) are seen grown out of clusters in different geometry; these growths are in repeated pattern. To fully obtain the dimensions of these structures an in-depth observation is carried out. The average length is estimated to be about 1.37 μm while the diameter at the tip is found to be approximately 15.03 nm. Fig 2(d), which shows the growth on coated Si(111), presents a "tetrahedral net" like structure of ZnO. The formation of the tetrahedral structure can be suggested to be originated from layered ZnO (double deposition or overgrowth). The distribution of this growth can simply be described as network of intertwined rods. Detail on the orientation of this structure is a work for further studies.

A vertically grown 2-D "nanowall" structure is observed for ZnO deposited on ITO substrate from zinc chloride solution (Fig. 2(e)). These nanowalls are found to be well distributed across the substrate, but each wall gets terminated in the lateral growth direction by another intercepting wall. These interceptions occur mostly at acute angle (less than 90^{o}). The average thickness of the wall is found to lie between 51 and 143 nm while the length varies from 443 nm to about 1.487 μm. The separation between the walls might not be absolutely well estimated within closed domain because of the hindrance of the growth in the lateral direction. While some gaps are found to be within 120nm and 300nm, some are found in excess of 700 nm. According to Pradhan & Leung 2008,[15] these variations are within the tolerance of suitable distinct walls that can offer high surface area appropriate for solar cell applications. Another deduction made here is the viability of zinc chloride precursor for nanowall synthesis. Most reported work on ZnO nanowalls has indicated the growth through zinc chloride solution or by introducing KCl (supporting electrolyte) into zinc nitrate solution. Elias *et al.*, 2010[6] have obtained different dimensions of urchin-like ZnO nanowalls by simply adjusting the concentration of $ZnCl_2$ and KCl solution. The nanowall structure reported by Pradhan & Leung[15] is obtained from a solution containing $Zn(NO_3)_2$ and 0.1M KCl supporting electrolyte. These evidences demonstrate the catalytic role of chloride ions in the formation of ZnO nanowalls.

Voltages and times reported in Table I represent the voltage at which the best ZnO nanostructure growth is obtained and the maximum time after which the reaction becomes not effective anymore. At the used concentration (0.2M), low voltages ($\sim$1.1 V, close to the values used in common

three-electrode cells), give no sign of ZnO nanostructures formation while at higher voltages (> 4 V) the deposition is extremely fast and not uniform, as shown by SEM not reported here. Looking at the table we can observe that the minimum voltage to get good growth is determined by the substrate, since using the same substrate, but changing the electrolyte, the required voltage is the same. This potential can be related to the sample conductivity. Supposing that Au-Cr/Si thin film resistivity is lower than the Si one because of the metal coating and that the ZnO coated Si(111) one is higher because of the high resistivity of the ZnO, we can say that the minimum growth voltage is determined by the conductivity of the substrate on which we want to grow the ZnO nanostructures: the highest it is, the lowest the required voltage to activate the reaction is. Deposition times are very similar for each preparation, except for the case in which an extra amount of Zn can be present on the substrate (Table I, d). This suggests a time dependence from the electrolyte concentration. Actually the only case in which the Zn amount is different is the one in which the coated Si is used. This substrate is covered by a thin ZnO film prepared using a procedure that could leave some extra Zn available for the ZnO production.

As a conclusion, the substrate influences the different agglomeration of the ZnO nanostructures, giving a morphological configuration, which is characteristic of each support, even if the electrolyte is the same. Furthermore, even changing the electrolyte, different growth morphologies are obtained using the same substrate. We can have a net of ZnO micro-crystals (Fig 2(d)), some round-shaped clusters (Fig 2(b)) or micro-structures all over the surface (Fig 2(a)–2(e)). Each of these structures can present different shapes: thin 2-D flakes on ITO and Au/Cr/ Si substrates and $Zn(NO)_3$ electrolyte (Fig 2(a) and 2(b)), bigger, more 3-D structures, Fig 2(c)–2(e). All of these structures have a common base, the typical wurtzite crystal structure of the ZnO crystal.

B. AFM

To complete the morphology studies on the grown ZnO nanostructures, we have observed some of our samples by AFM, for a direct evaluation of surface roughness.

In particular, in Fig 3, AFM images on corals (a), nanowalls (b) and nanorods (c) structures are shown. The statistical analysis of the images returns the following values regarding the average height (h) with respect to the substrate's surface and the roughness (RMS): h $= 0.5$ μm and RMS $=$ 187.8 nm for corals, h $= 120$ nm and RMS $= 19.1$ nm for nanowalls, h $= 0.7$ μm and RMS $= 333.3$ nm for nanorods. The highest roughness is measured in the case of nanorods like sample, which forms a not so dense pattern as it is the case of the nanowalls. The nanorods agglomerates form a net leaving deep and wide holes in between the ZnO macro-structure in which the substrate is still visible. On the contrary the nanowalls sample, even if the walls are standing up with respect to the substrate, they are very dense packed and form a compact layer, making the substrate almost not accessible by the AFM probe, reducing in this way the resulting roughness of the surface.

Even if the minimum voltage to get ZnO nanostructures seems to be determined by the conductivity of the substrate, the applied voltage and deposition time play a major role on growth structures. If we compare samples obtained from zinc nitrate solution under approximate equal conditions in concentration and pH, we see that samples in Fig 2(a)–2(c) are obtained at nearly the same deposition time, but with varying applied voltage. As the applied voltage increases the growth height increases. This trend is also observed in samples prepared using the zinc sulfate as electrolyte, results not shown here, though considerably higher voltage are required, probably because of a different potential necessary to activate the reaction. We cannot determine the height of the nanostructures in Fig 2(d) due to its excessive roughness. Looking at ZnO nanowalls in Fig 2(e) we see that the deposition takes a longer time (see Table I) when compared with the formation of corals in Fig 2(a), where the same voltage and substrate are used. This can be attributed to the nature of the electrolyte.

C. XRD

To examine the purity and crystallinity of the samples, we selectively carry out XRD experiments on two samples (corals (Fig 2(a)) and nanorods (Fig 2(c))) prepared under the same conditions. This enables to compare without ambiguity our observations with literature. The diffraction patterns for

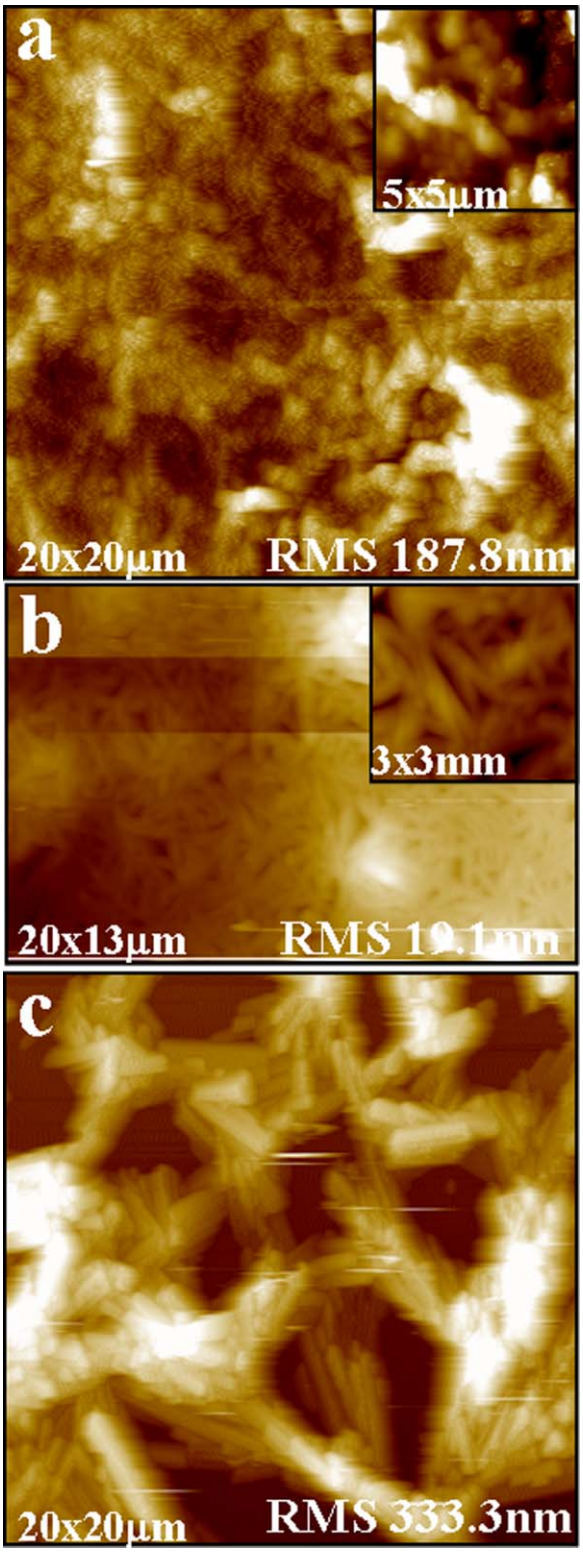

FIG. 3. AFM images of corals (a), nanowalls (b), nanorods (c)

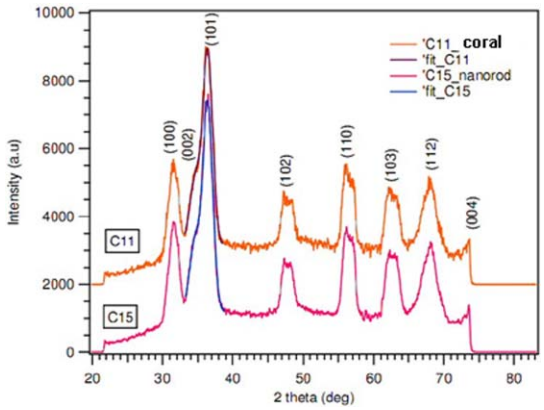

FIG. 4. XRD measurements of "corals" and "nanorods" samples shown in Fig 2. The diffraction peaks are sharp and strong and well indexed to the hexagonal phase of the wurtzite structure (space group $P6_3mc$), according to the values of standard XRD ZnO pattern found in the International Centre for Diffraction Database (ICDD)

both samples are shown in Fig 4. It can be seen immediately that the diffraction peaks are sharp, strong and well indexed to the hexagonal phase of wurtzite structure (space group $P6_3mc$), according to the values of standard XRD ZnO pattern found in the International Centre for Diffraction Database (ICDD).[18] No peaks of any other phase were detected, indicating that the ZnO samples are highly pure. The sharp peaks indicate furthermore that the samples are well crystallized. From the full width at half maximum (FWHM) of each peak, which is obtained by fitting them with Gaussian functions, and using the Scherrer's formula[19] we can give an average value of the size of the crystalline particles. The result is somewhat under-estimated because we did not correct the data for the instrumental broadening. But still we can say that the crystallite size is, both for the building units of the corals and the nanorods, $\sim$ 5 nm. This result corresponds very well with the ZnO crystallite sizes obtained by other production techniques.[20–22] The interplanar spacing d_{hkl} were determined for plane (101) using the principle of Bragg's reflection. The values obtained for each crystal, $\sim$2.47 Å compare well with the values of ICDD (2.47 Å). These data confirm the good quality of the grown sample from the point of view of crystallinity.

D. XPS

To further substantiate the quality of our samples, we perform core level photoemission spectroscopy experiments on few samples (samples shown in Fig 2(a), 2(c), and 2(e)) to check the stoichiometry and the purity of the ZnO nanostructures. Survey spectra, not shown here, are collected at Micro & Nano Carbon Laboratory. They present no contaminants due to residuals from the electro-deposition process for the samples where the $Zn(NO_3)_2$ electrolyte is used, while for those where the $ZnCl_2$ is used, a low amount of Cl is present on the surfaces. In general only oxygen, zinc and a low amount of amorphous carbon is detected. At ALOISA beamline, high-resolution spectra are collected for Zn2*p* and O1*s* signal on corals and nanorods (Fig 2(a) and 2(c)). XPS spectra are shown in Fig 5. The binding energy alignment of all spectra is done by fixing the $Zn2p_{3/2}$ at 1022.5 eV according to the value found in literature.[25]

The O1*s* spectrum of both samples clearly presents at least two components. To understand the origin of these components, the spectra are fitted using Gaussian functions. Fig 5(a) shows the O1*s* spectrum of the nanorods and the relative fitting curves. A major component appears at binding energy 531.3 eV, which is peculiar of the O-Zn bond (ZnO), while a small shoulder appears at higher binding energy, 532.7 eV. A second component is observed also by Pradahan *et al.*,[23] which they associate to the zinc hydroxide, $Zn(OH)_2$, and by many other authors.[24,25] The energy difference between the two components in our case is 1.4 eV, which represents a smaller value than the ones reported in literature between 1.5-2 eV. In our case it is unlikely that the component is related to the hydroxyl groups because the sample is annealed at 300 °C, *in situ*, before the photoemission

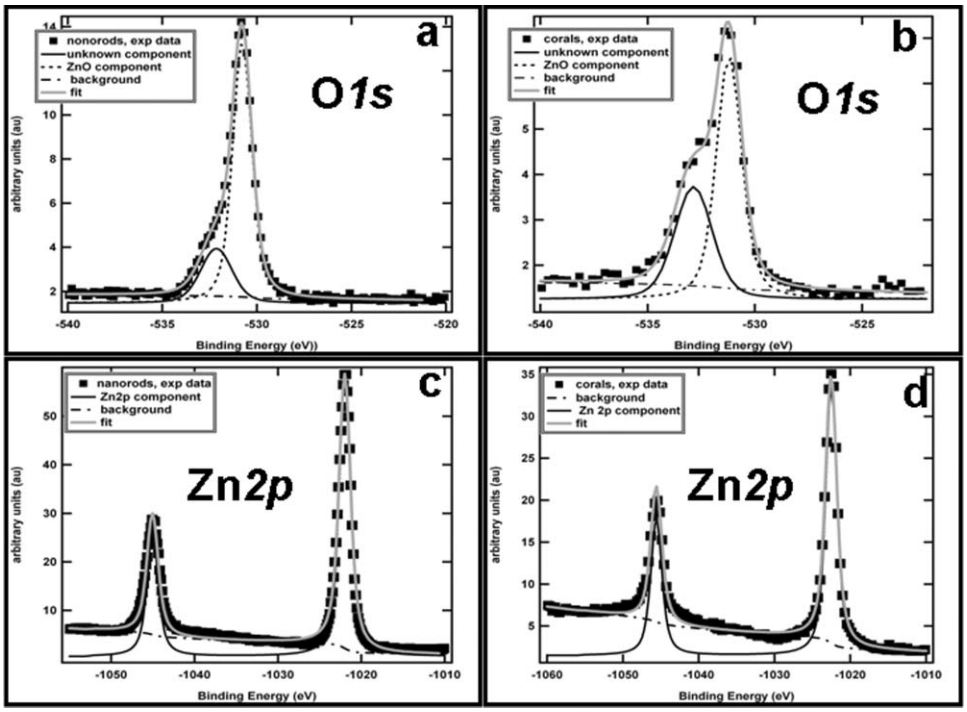

FIG. 5. Zn2p and O1s XPS spectra of "nanorods" (a, c) and "corals" (b, d). Both samples are annealed at 300°C, in situ, before XPS measurements. Both of them present two O1s components, but only the major one can be certainly assigned to the ZnO.

measurements, causing desorption of these groups, which happens at 200 °C.[28] We perform also a quantitative analysis by calculating the total areas of Zn2*p* (Fig 5(c)) and O1*s* signal. Taking into account element cross sections and analyzer transmissions at the different kinetic energies at which the two signals are collected, it results in a Zn : O = 1 : 4.7 ratio, suggesting the presence of an extra amount of oxygen. The right stoichiometry should be Zn : O = 2 : 3, considering both ZnO and the hydroxyl $Zn(OH)_2$ since it's not possible to distinguish in the Zn2*p* spectra the ZnO and hydroxyl components. Further photoluminescence experiments on these nanostructures are necessary to confirm the presence of extra oxygen and its origin. Actually according to the literature the energy emission range is different depending on the defects, like excess of oxygen at interstitial defects, and hydroxyl groups.[26,27]

The corals O1*s* spectrum (Fig 5(b)) shows at least two components. If we fit the spectrum in the same way done for the nanorods and we do the same quantitative analysis, we don't get a Zn : O = 2 : 3 ratio, as it should be in presence of ZnO and hydroxyl, but Zn : O = 1 : 4.9. This means that a further extra amount of oxygen is present also on this sample. As in the previous case the sample is annealed at 300 °C, *in situ*, before the photoemission experiments, therefore the $Zn(OH)_2$ component should not be present. Even if in this case another component could be present on the spectrum, i.e. the oxygen from ITO substrate at 532 eV,[28] we believe that this oxygen component is not detected during the measurements shown in Fig 5. Actually, the ALOISA beamline has a very grazing photon beam setup (6° of incidence angle), which allows an extremely surface sensitive measurements. All of this brings to the conclusion that the grown ZnO, even if it shows a good crystallinity, is characterized by defects where extra oxygen atoms can be trapped.

IV. CONCLUSION

A simple two-electrode electrochemical cell is used to grow zinc oxide nanostructures at room temperature. The results and analysis of the morphology demonstrate the ease and flexibility of this cell to grow diverse nanostructures based on semiconducting compounds on conductive substrates

from electrolytic solution. The growth distribution reveals the influence of substrate properties on the morphology of the ZnO clusters. It is found that high concentration of the starting solution (above 0.01M mostly earlier reported) with non-catalytic process can be adopted to produce stable ZnO at fast growth rate, while relative high voltages are required at the cathode to compensate for the non-inclusion of the third electrode in our cell arrangement. Diffraction data have shown a good crystallinity of the samples: the typical hexagonal wurtizite structure of ZnO according to ICDD, while photoemission experiments have shown the purity of the sample from a chemical point of view, but the presence of defects characterized by an oxygen excess.

ACKNOWLEDGMENT

This work is supported by the Abdus Salam ICTP/IAEA and Sincrotrone Trieste, Italy where it was majorly carried out. The supports of Materials Science division, CERD-OAU Ile-Ife, Nigeria are appreciated.

[1] K. J. Choi and H. W. Jang, Sensors **10**, 4083 (2010); D. M. Bagnall, Y. F. Chen, Z. Zhu, T. Yao, S. Koyama, M. Y. Shen and T. Goto, Appl. Phys. Lett. **70**, 2230 (1997); R. Jose, V. Thavasi and S. Ramakrishna, J. Am. Ceram. Soc. **92**, 289 (2009); X. W. Sun and J. X. Wang, Nanoletters **8**, 1884 (2008).
[2] M. Izaki, T. Shinagawa, and H. Takahashi, J. Appl. Phys. D. **39**, 1481 (2006).
[3] Z. L. Wang, X. Y. Kong, Y. Ding, P. X. Gao, W. L. Hughes, R. S. Yang and Y. Zhang, Adv. Funct. Mat. **14**, 943 (2004).
[4] Zhou Li, Rusen Yang, Min Yu, Fan Bai, Cheng Li and Zhong Lin Wang, J. Phys. Chem. C **112**, 20115 (2008).
[5] D. C. Look, D. C. Reynolds, J. W. Hemsky, R. L. Jones and R. Sizelove, Appl. Phys. Lett **75**, 811 (1999).
[6] C. Xu, M. Kim, J. Chun and D. E. J. Kim, Nanotechnology **16**, 2104 (2005); J. Elias, C. L. Clement, M. Bechelany, J. Michler, G. Y Wang, Z. Wang and L. Philippe, Adv. Mat. **22**, 1607 (2010).
[7] Z. L. S. Seow, A. S. W. Wong, V. Thavasi, R. Jose, S. Ramakrishna and G. W. Ho, Nanotechnology **20**, 045604 (2009).
[8] M. Izaki, T. Omi, Appl. Phys. Lett. **68**, 2439 (1996).
[9] S. Peulon and D. Lincot, Adv. Mat. **8**, 166 (1996).
[10] R. Tena-Zaera, J. Elias, C Levy-Clement, C. Bekeney, T. Voss, I. Mora-Sero and J. Bisquert, J. Phys. Chem. C **112**, 16318 (2008).
[11] Sung Joong Kim, Hee-Gyoo Kang, Jinsub Choi, Current Appl. Phys. **10**, 740 (2010).
[12] Zhuo Zhang, Guowen Meng, Qiaoling Xu, Yemin Hu, Qiang Wu and Zheng Hu, J. Phys. Chem. C **114**, 189 (2010).
[13] M. S. Boeckl, A. L. Bramblett, K. D. Hauch, T. Sasaki, B. D. Ratner and J. W. Rogers Jr, Langmuir **16**, 5644 (2000).
[14] B. Ingham, B. N. Illy, M. F. Toney, M. L. Howdyshell and M. P. Rayan, J. Phys. Chem. C **112**, 14863 (2008).
[15] Debabrata Pradhan and Kam Tong Leung, Langmuir **24**, 9706 (2008).
[16] Pu Xian Gao, Chang Shi Lao, Yong Ding and Zhong Li Wang, Adv. Funct. Mat. **16**, 53 (2006).
[17] Waldo J. E. Beek, Lenneke H. Slooff, Martijn M. Wienk, Jan M. Kroon and Rene' A. J. Janssen, Adv. Funct. Mat. **15**, 1703 (2005).
[18] JCPDS International Center For Diffraction Data, *Powder Diffraction File 01-076-0704*, PA: Swarthmore, (1991).
[19] L. S Birks and H. Friedman, J. Appl. Phys. **17**, 687 (1946).
[20] R. Viswanatha, H. Amenitsch, D. D. Sarma, J. Am. Chem. Soc. **129**, 4470 (2007).
[21] M. S. Tokumoto, S. H. Pulcinelli, C. V. Santilli, A. F. J. Craievich, Non-Cryst. Solids **247**, 176 (1999).
[22] M. Bitenc, P. Podbrščček, Z. Crnjak Orel, P. Dubček, S. Bernstorff, B. Orel, G. Dražič, to be submitted.
[23] Debabrata Pradhan, Mukul Kumar, Yoshinori Ando, and K. T. Leung, Appl. Materials. & Interfaces. **1**, 789 (2009).
[24] M. K. Puchert, P. Y. Timbrell and R. N. Lam, J. Vac. Sci. Technol. A **14** (4), 2220 (1996).
[25] L. Zhang, D. Wett, R. Szargan and T. Chasse', Surf. Int. Anal. **36**, 1479 (2004).
[26] A. B. Djurisic, Y. H. Leung, K. H. Tam, Y. F. Hsu, L. Ding, W. K. Ge, Y. C. Zhong, K. S. Wong, W. K. Chan, H. L. Tam, K. W. Cheah, W. M. Kwok and D. L. Phillips, Nanotechnology **18**, 095702 (2007).
[27] Xiang Liu, Xiaohua Wu, Hui Cao, and R. P. H. Chang, J. Appl. Phys **95**, 3141 (2004).
[28] S. K. So, W. K. Choi, C. H. Cheng, L. M. Leung and C. F. Kwong, Appl. Physics A **68**, 447 (1999).